Supplementary materials for:

Amygdala to nucleus accumbens excitatory transmission facilitates reward seeking

Garret D. Stuber[1,2*], Dennis R. Sparta[1,2], Alice M. Stamatakis[1], Wieke A. van Leeuwen[2], Juanita E. Hardjoprajitno[2], Saemi Cho[2], Kay M. Tye[2], Kimberly A. Kempadoo[2], Feng Zhang[3], Karl Deisseroth[3], Antonello Bonci[2,4]

[1]Departments of Psychiatry & Cell and Molecular Physiology
UNC Neuroscience Center
University of North Carolina at Chapel Hill
Chapel Hill, NC USA

[2]Ernest Gallo Clinic and Research Center
Department of Neurology
Wheeler Center for the Neurobiology of Drug Addiction
University of California San Francisco
San Francisco, CA USA

[3] Departments of Bioengineering and Psychiatry and Behavioral Sciences
Stanford University, Stanford, CA USA

[4]Intramural Research Program
National Institute on Drug Abuse
Baltimore, MD USA

[*]Address correspondence to:

Garret D. Stuber, Ph.D.
Assistant Professor
Departments of Psychiatry & Cell and Molecular Physiology
UNC Neuroscience Center
University of North Carolina at Chapel Hill
Tel: +1 (919) 843-7140
Fax: +1 (919) 966-1050
Email: gstuber@med.unc.edu

Materials and methods:

Experimental subjects and stereotaxic surgery. Adult (25-30g) male C57BL/6J mice (Jackson Laboratory, Bar Harbor, ME) were group-housed until surgery. Mice were maintained on a 12:12 light cycle (lights on at 07:00). Once the animals were acclimated to the animal facility for ~1 week, they were anesthetized with 150 mg/kg ketamine 50 mg/kg xylazine and placed in a stereotaxic frame (Kopf Instruments). Microinjection needles were then inserted bilaterally directly above the BLA (coordinates from Bregma: -1.6 AP, ±3.1 ML, -4.9 DV). Microinjections were performed using custom-made injection needles (26 gauge) connected to a 2 µl Hamilton syringe. Each BLA was injected with 0.3 – 0.5 µl of purified and concentrated AAV (~10^{12} infectious units/mL) coding ChR2-EYFP, NpHR3.0-EYFP, or EYFP under control of the CaMKIIα promoter over 10 minutes followed by an additional 10 minutes to allow diffusion of viral particles away from the injection site. For optical self-stimulation experiments mice were first injected unilaterally in the BLA with virus and then a guide cannula was implanted directly over the ipsilateral NAc (+1.3 AP, ±1.0 ML, -4.0 DV) to allow for insertion of the fiber optic cable during the experiment, which was secured to the skull using Geristore (www.denmat.com) dental cement. Mice were then returned to their home cage. Body weight and signs of illness were monitored until recovery from surgery (approx. 2 weeks). All procedures were conducted in accordance with the Guide for the Care and Use of Laboratory Animals, as adopted by NIH, and with approval of the UNC and UCSF Institutional Animal Care and Use Committees.

Construct and AAV preparation. DNA plasmids coding pAAV-CaMKIIα-ChR2-EYFP (H134R), pAAV-CaMKIIα-NpHR3.0-EYFP, or pAAV-CaMKIIα-EYFP were obtained from the laboratory of Karl Deisseroth (see www.optogenetics.org for additional details). Plasmid DNA

was amplified, purified, and collected using a standard plasmid maxiprep kit (Qiagen). Following plasmid purification, restriction digest, and sequencing to assure DNA fidelity, purified recombinant AAV vectors were serotyped with AAV5 coat proteins and packaged using calcium phosphate precipitation methods by the UNC Vector Core facilities (University of North Carolina, Chapel Hill). The final viral concentration was 1-2 x 10^{12} genome copies/mL.

Slice preparation for patch-clamp electrophysiology. Mice were anesthetized with pentobarbital and perfused transcardially with modified aCSF containing (in mM): 225 sucrose, 119 NaCl, 2.5 KCl, 1.0 NaH_2PO_4, 4.9 $MgCl_2$, 0.1 $CaCl_2$, 26.2 $NaHCO_3$, 1.25 glucose. The brain was removed rapidly from the skull and placed in the same solution used for perfusion at ~0°C. Coronal sections of the NAc or BLA (200 µm) were then cut on a vibratome (VT-1200, Leica Microsysytems). Slices were then placed in a holding chamber and allowed to recover for at least 30 min before being placed in the recording chamber and superfused with bicarbonate-buffered solution saturated with 95% O2 and 5% CO_2 and containing (in mM): 119 NaCl, 2.5 KCl, 1.0 NaH_2PO_4, 1.3 $MgCl_2$, 2.5 $CaCl_2$, 26.2 $NaHCO_3$, and 11 glucose (at ~32°C).

Patch-clamp electrophysiology. Cells were visualized using infrared differential interference contrast and fluoresce microscopy. Whole-cell voltage-clamp or current clamp recordings of BLA and NAc neurons were made using an Axopatch 200A or B amplifier. Patch electrodes (3.0 - 5.0 MΩ) were backfilled with internal solution containing 130 mM KOH, 105 mM methanesulfonic acid, 17 mM hydrochloric acid, 20 mM HEPES, 0.2 mM EGTA, 2.8 mM NaCl, 2.5 mg/ml MgATP, and 0.25 mg/ml GTP (pH 7.35, 270–285 mOsm). Series resistance (15 - 25 MΩ) and/or input resistance were monitored online with a 4 mV hyperpolarizing step (50 ms) given between stimulation sweeps. All data was filtered at 2 kHz, digitized, and collected using

pClamp10 software (Molecular Devices). For current clamp experiments to characterize cell firing, 10 pulses at frequencies of 1, 5, 10, and 20 Hz, respectively, were tested to determine spike fidelity (the percentage of light pulses that lead to action potentials). For optical stimulation of EPSCs, stimulation (pulses of 1 - 2 mW, 473 nm light delivery via a 200 μm optical-fiber coupled to a solid-state laser) was used to evoke presynaptic glutamate release from BLA projections to the NAc. NAc MSNs were voltage-clamped at -70 mV. For pharmacological characterization of glutamate currents, light-evoked EPSCs were recorded for 10 min followed by bath application of 10 μM CNQX for an additional 10 min. 10-12 sweeps pre- and post-drug were averaged and peak EPSCs amplitudes were then measured. For EPSC pulse train experiments, input-specific currents were evoked by 60 optical pulses (20 Hz stimulation, 5 ms pulse duration.). This was repeated 12 times at 0.1 Hz. 4 μM SCH23390 or vehicle was then bath applied for 10 min and the stimulus train was again repeated. The average EPSC train from the 6 sweeps immediately prior to drug application and those for the 6 sweeps immediately after drug application were then compared.

In vivo optrode recording. Approximately, 21 – 28 d after bilateral AAV-CaMKIIα-ChR2-EYFP injection into the BLA, mice were deeply anesthetized with ketamine/xylazine and placed in a stereotaxic frame equipped with a temperature controller to regulate body temperature. The skull was then removed directly above the NAc. Parylene coated tungsten electrodes (1 MΩ), epoxied to an optical fiber 200 μm core diameter, 0.37 N.A.) coupled to a 473 nm laser were then lowered into the NAc to record unit activity of postsynaptic MSNs following trains of light pulses used to evoke BLA-to-NAc-specific glutamate release. Ten pulses of light (10 - 20 mW, 5 ms) at frequencies of 1, 5, 10, and 20 Hz, respectively, were used to determine spike fidelity *in vivo* analogous to what was with performed during whole-cell recording. Unit activity was

amplified with an extracellular amplifier (A-M systems), band-pass filtered at 300Hz low/5 kHz, and digitized using pClamp10 software.

Freely moving optical self-stimulation. 21 – 28 d following injection of pAAV-CaMKIIα-ChR2-EYFP or control virus into the BLA, mice with cannula placed above the NAc were prepared for nosepoke training. Mice were mildly food restricted to four grams of food per day to stabilize body weight and facilitate behavioral responding. Body weight was monitored throughout the experiment and did not fall below ~90% of their free feeding weight. Immediately before placing mice in the operant chambers, stylets were removed from the cannula, and a flat cut 125 μm diameter fiber optic cable, coupled to a solid state 473 nm laser outside of the operant chamber, was inserted through the guide cannula and placed directly above the NAc. Immediately prior to insertion, through the guide cannula, light output through the optical fibers was adjusted to 10 - 20 mW. The optical fiber was then secured into place via a custom-made locking mechanism to ensure no movement of the fiber occurred during the experiment. Mice were then placed in standard Med-Associates operant chambers equipped with an active and inactive nosepoke operandum directly below two cue lights. The chambers were also equipped with house lights, audio stimulus generators, and video cameras coupled to DVD recorders. A one hour optical self-stimulation session began with the onset of the cue light above the active nosepoke operandum. Each active nosepoke performed by the animal resulted in an optical stimulation of BLA-to-NAc fibers (60 pulses, 20 Hz, 5 ms pulse duration). Both active and inactive nosepoke timestamp data was recorded using Med-PC software and analyzed using Neuroexplorer and Microsoft Excel software.

NAc microinjections prior to optical self-stimulation. Stylets were removed from guide cannula and a 26-gauge injector needle connected to a 1 µL Hamilton syringe was inserted. All microinjections were delivered in 0.3 µl sterile saline at a rate of 0.1 µl/min. Injector needles remained in place for an additional 2 min before being removed and replaced immediately with wither stylets or optical fibers for self-stimulation sessions. Doses of drugs used for microinjections were: 600 ng/0.3 µl for SCH23390; 100 ng/0.3 µl and 3 µg/0.3 µl for raclopride, and 10 ug/0.3 µl for lidocaine.

Implantable optical fibers for NpHR inhibition during behavior. For these experiments, mice were bilaterally injected into the BLA with virus coding for NpHR3.0-EYFP or EYFP as described above. Mice were also implanted with bilateral optical fibers targeted directly above each NAc. Optical fibers were constructed in-house by interfacing a 7 – 10 mm piece or 200 µm, 0.37 NA optical fiber with a 1.25 mm zirconia ferrule (fiber extending 5 mm beyond the end of the ferrule.) Fibers were epoxied into ferrules, and cut and polished. After construction, all fibers were calibrated to determine a percentage of light transmission at the fiber tip that would interface with the brain. Prior to bilateral implantation, fibers were matched to each other so that each fiber output equal amounts of light (within 10%). This was done to ensure that an equal amount of light was delivered to each hemisphere. Following surgery, protective plastic caps were placed on the implanted optical fibers to protect them from dust and debris.

Four to five weeks after implantation surgery and three days prior to the experiment, mice were connected to 'dummy' optical patch cables each day for 30 – 60 min to habituate them to the tethering procedure in their home cage. On experiment days, protective caps were removed from the implanted fibers. Fibers were then connected to custom-made optical patch cables (62.5 µm core diameter) that were covered with furcation tubing to protect the cables and

prevent light from the laser from illuminating the operant chamber. Bilateral fibers were connected to a fiber splitter (50:50 split ratio) that interfaced with a fiber-coupled 532 nm DPSS laser (200 mW). Based on each pair of fibers' calibration factor, light intensity was set to 10 mW illumination at each fiber tip in the brain.

Optical inhibition of BLA-to-NAc fibers during sucrose responding. Mice with optical fibers implanted above the NAc and expressing either NpHR3.0-EYFP or EYFP in BLA-to-NAc fibers were trained to drink sucrose in response to an environmental stimuli that predicted sucrose delivery. The start of the session was signaled by the onset of white noise in the operant chamber. Each session consisted of 50 cue-reward pairings with a random inter-trial interval of 120 s. During each trial, a TTL was sent from the behavioral hardware to engage the laser 200 ms prior to the onset of a 5 s reward-predictive stimulus (tone/house light compound stimulus). Delivery of 20 µl of 20% sucrose to a receptacle occurred immediately after the termination of the reward-predictive cue, and the laser pulse was terminated 200 ms after cue offset. Starting and extending the laser pulse 200 ms before and after the cue were done based on *in vitro* experiments where we observed that activation of NpHR led to maximal inhibition 200 ms after the start of the laser pulse. Cue presentation, reward delivery, lick, and laser timestamps were stored as separate data arrays and analyzed offline with Microsoft Excel and Neuroexplorer.

Timelocked licking behavior was quantified for all mice. Mice that did not make at least 200 licks on at least one of the four conditioning sessions were excluded from analysis. This resulted in the removal of n = 2 NpHR and n = 2 EYFP mice from analysis. Timelocked lick histograms with 0.5s time bins were then constructed from -10 – 30 s timelocked to cue onset (t = 0). Lick rates were normalized to baseline periods using a z-score procedure ($z = (x - \mu)/ \sigma$)

where the μ was the average lick rate and σ was the standard deviation in the 10 s preceding the cue onset.

Optical inhibition of BLA-to-NAc fibers and conditioned place preference/aversion. The same mice used in the cue-evoke sucrose intake experiment were tested 1 – 2 weeks later in a modified conditioned place procedure to assay whether optical inhibition of BLA-to-NAc fibers resulted in a place preference or aversion. On day 1, all NpHR and EYFP mice underwent a 25 min pre-test where mice were allowed to explore two contextually distinct compartments to determine whether there was an innate preference to one side of the chamber. Mice then underwent two 30 min conditioning sessions over the next two days where one distinct environment was paired with either no stimulation (but still tethered to optical fibers) or the other environment where mice received a 5 s laser pulses delivered to the NAc every 90 s. Stimulation and no stimulation were counter-balanced across mice. Following conditioning sessions, mice underwent a final preference test (25 min) where they again had access to both sides of the chamber. To examine differences in preference or aversion in NpHR vs. EYFP mice, the amount of time spent on the side where mice received laser pulses was normalized to the amount of time they spent on that side during the pre-test session. Percentage of time spent on the stimulation-paired side was then compared between NpHR and EYFP groups.

Data analysis. Statistical significance was assessed using t-tests or analysis of variance (ANOVA) followed by post-hoc tests when applicable using an $\alpha = 0.05$. Data was analyzed using Microsoft Excel with the Statplus plugin and Prism (GraphPad Software).

Virus expression and histology. Following behavioral experiments, mice were deeply anesthetized with pentobarbital and perfused transcardially with phosphate buffered saline (PBS) followed by 4% paraformaldehyde (PFA) dissolved in PBS. Brains were removed carefully and post-fixed in 4% PFA for an additional 24 - 48 hrs. Brains were transferred to 30% sucrose for 48 – 72 hrs before slicing 50 µm sections of the BLA or NAc on a freezing stage microtome or cryostat. Slices were then triple washed in PBS for 5 min. Slices were then stained with 2% Neurotrace fluorescent Nissl stain (Invitrogen; excitation 530 nm, emission 615 nm) diluted in PBS with 0.1% Triton X-100, for 1 hr. Slices were then washed and mounted on gelatin-coated slides, treated with fluorescent-mounting media, and coverslipped. Expression of ChR2-EYFP, NpHR3.0-EYFP, or EYFP was then examined for all mice using either a Nikon inverted fluorescent microscope with a 4, 10, or 20X objective or a Zeiss laser-scanning confocal microscope at 25 and 63X. Following injection of virus into the BLA, robust expression of ChR2-EYFP was observed in BLA projection targets including the NAc, mPFC, hippocampus, insular cortex, and to a lesser extent, the dorsal medial striatum. Mice showing no EYFP expression in the NAc due to faulty microinjections or mice showing cannula or fiber placements outside of the NAc were excluded from analysis.

Reconstruction of optical stimulation or inhibition sites in the NAc. To determine optical stimulation sites in experiments where guide cannulas were used to introduce optical fibers into brain tissue (BLA-to-NAc and mPFC-to-NAc optical self-stimulation experiments, see **Supplementary Figs. 3,14** for location of optical stimulation sites), fixed and stained coronal brain sections (see above) containing the NAc and cannula tracks were examined on an upright conventional fluorescent microscope. Cannula tracks were located in the slices and optical stimulation sites were determined by locating the site 1 mm ventral to the end of the cannula tip. A 1 mm distance was used in these experiments because the optical fibers extended 0.5 mm

beyond the end of the cannula (each fiber was cut to this length prior to insertion). Based on light output from these optical fibers (477 mW*mm^{-1} at the tip and calculating intensity taking into account geometric loss and scattering through tissue[1] loss at 0.5 mm beyond the fiber tip led to an estimated 2.6% transmission or 12.4 mW*mm^{-1} at this distance. At 1 mm from the tip of the optical fiber, estimated transmission dropped to 0.56% or 2.67 mW*mm$^{-1,}$ which approximates the minimum intensity required to activate opsin proteins (1 mW*mm^{-1}). For NpHR-mediated inhibition experiments, optical inhibition sites (**Supplementary Fig. 11**) were determined in a similar fashion; with 0.5 mm used as the distance from fiber tip to the diagrammed inhibition sites, as no guide cannula was present. 0.5 mm beyond the optical fiber tip represents the center location where optical stimulation or inhibition occurs, (0.5 mm above and below). All calculations were performed using equations and constants listed in Aravanis et al., 2007[21].

References:

[21] Aravanis, A.M., *et al.* An optical neural interface: *in vivo* control of rodent motor cortex with integrated fiberoptic and optogenetic technology. *J Neural Eng* **4**, S143-156 (2007).

Stuber et al., Supplementary Figure 1

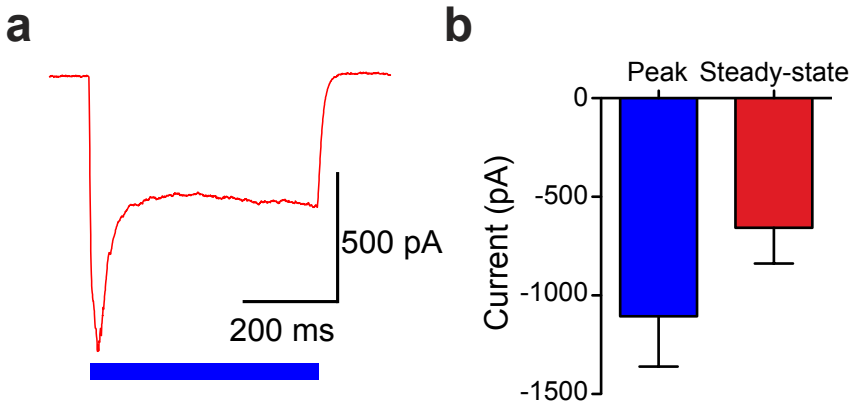

Suppplementary Figure 1: ChR2 mediated currents recorded from BLA neurons. **a**, Voltage-clamped BLA neurons at -70 mV respond to a 500-ms pulse of 473 nm. **b**, average data for all recorded cells (peak current: -1105 ± 255 pA; steady-state current: -656.9 ± 181 pA; P = 0.16; n = 10 cells).

Stuber et al., Supplementary Figure 2

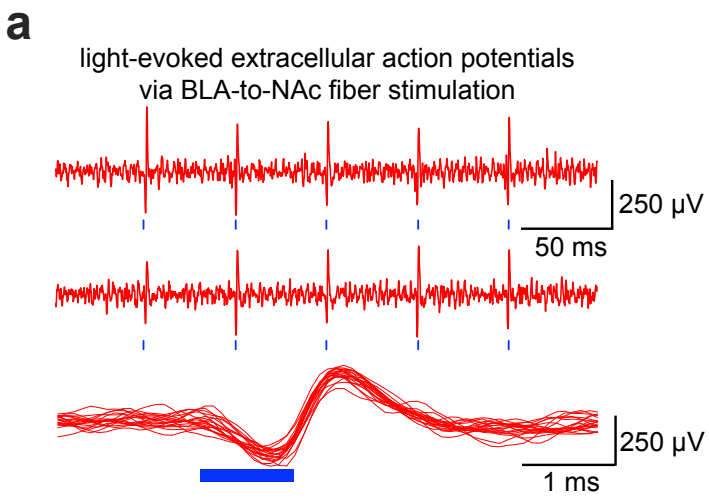

Supplementary Figure 2: Optical stimulation of BLA-to-NAc fibers results in post-synaptic action potentials *in vivo*. a, *In vivo* optrode recordings of action potentials from NAc neurons following optical stimulation of BLA-to-NAc fibers. Lower trace shows expanded extracellular waveforms from a single neuron.

a

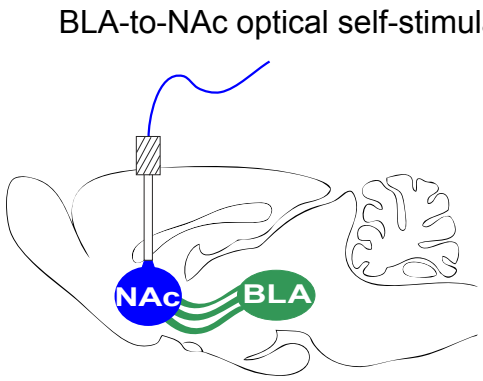

b

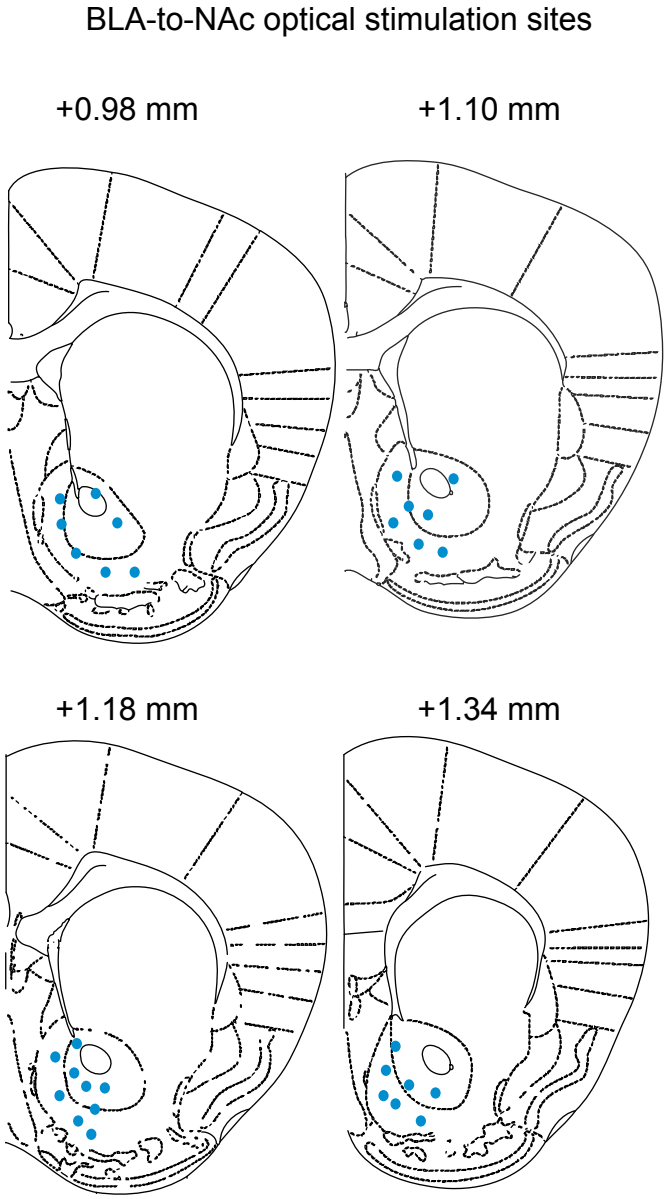

Supplementary Figure 3: Optical stimulation sites for BLA-to-NAc mice. a, An optical fiber is inserted through a guide cannula into the NAc to activate BLA-to-NAc ChR2-expressing fibers. **b**, Diagram of optical stimulation sites located 1mm from the cannula tip locations for ChR2-EYFP and EYFP mice used in BLA-to-NAc stimulation experi-

Stuber et al., Supplementary Figure 4

a

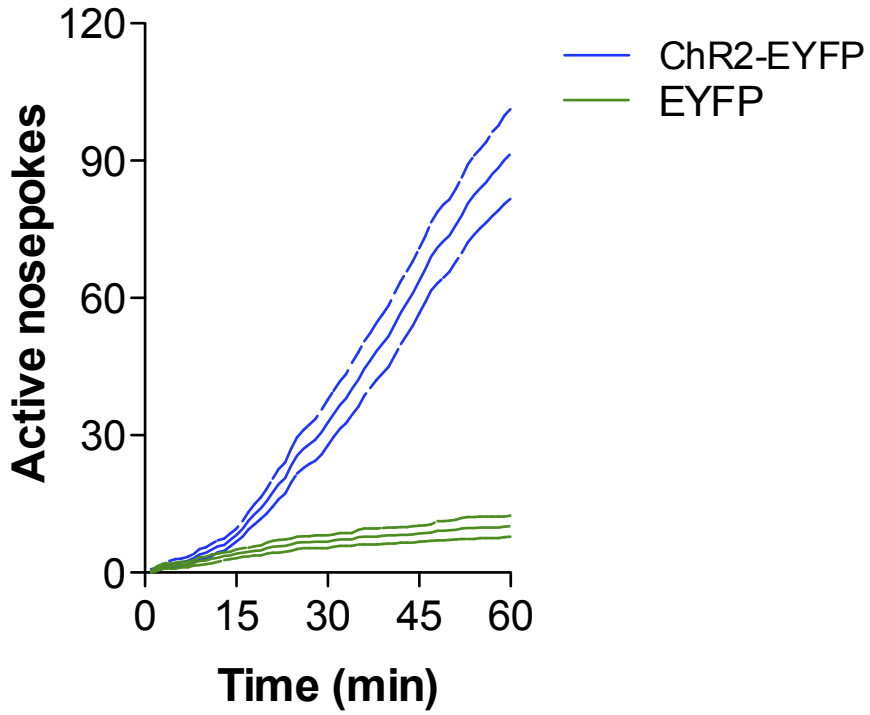

Supplementary Figure 4: Average cumulative nosepokes of BLA-to-NAc mice. a, Average cumulative records for active nosepokes of mice expressing ChR2-EYFP or EYFP in BLA-to-NAc fibers.

Stuber et al., Supplementary Figure 5

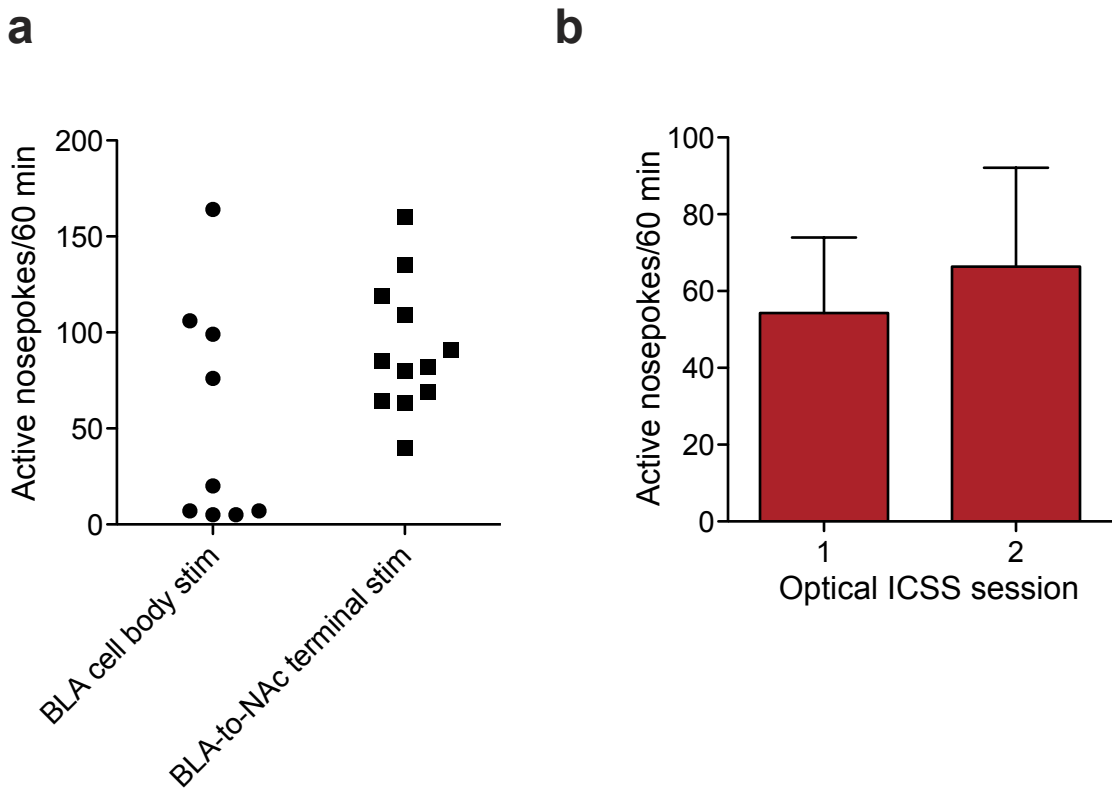

Supplementary Figure 5: Direct optogenetic activity of BLA cell bodies leads to variable self-stimulation behavior. **a,** Mice injected with AAV-CaMKIIa-ChR2-EYFP into the BLA and implanted with guide cannula directly above the BLA were tested for optical self-stimulation behavior. While all mice showed robust ChR2-EYFP expression, only 4/9 mice tested showed self-stimulation behavior. This is shown in comparison to a cohort of BLA-to-NAc stimulation mice. **b**, Average active nosepokes made by mice receiving BLA cell body stimulation across two consecutive behavioral sessions.

Stuber et al., Supplementary Figure 6

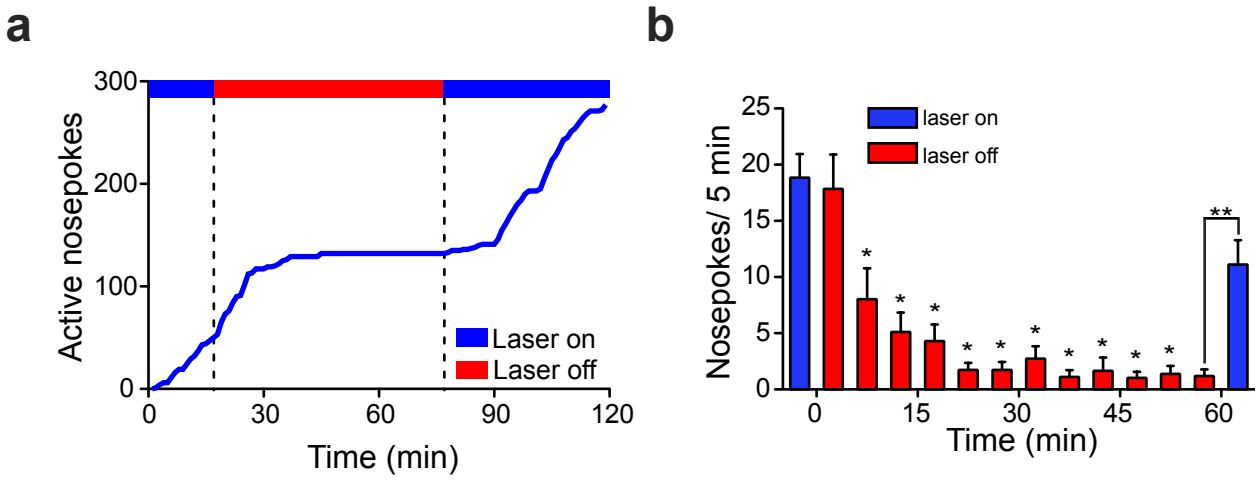

Supplementary Figure 6: Behavioral responding during extinction and renwel of BLA-to-NAc optical self-stimulation. Example cumulative nosepokes from a single mouse diminish in the absence of laser stimulation. **b**, Average active nosepokes are reduced in the absence of laser stimulation (n = 11 mice; $P < 0.0001$).

Stuber et al., Supplementary Figure 7

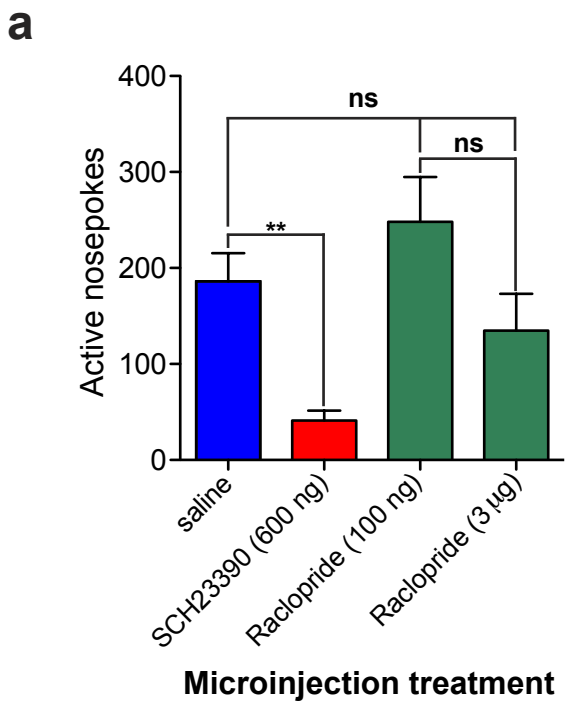

Supplementary Figure 7: Intra-NAc D1R receptor antagonism blocks BLA-to-NAc self-stimulation. **a**, Average number of active nosepokes made for BLA-to-NAc stimulation in mice treated with SCH23390 or raclopride. Both moderate and high doses of raclopride were ineffective at blocking BLA-to-NAc self-stimulation behavior, and therefore Raclopride microinjection data at both doses were pooled.

Stuber et al., Supplementary Figure 8

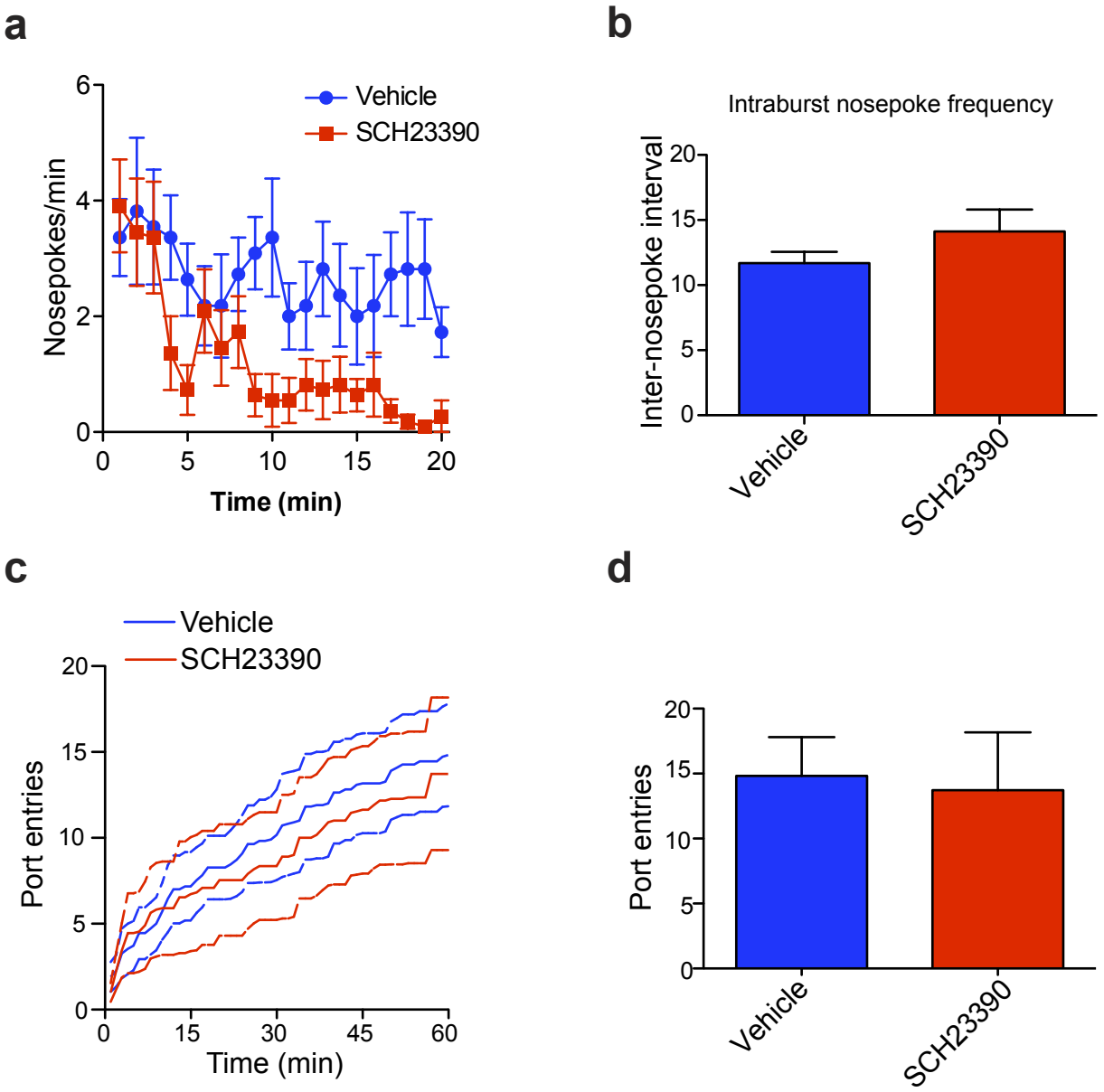

Supplementary Figure 8: Unilateral intra-NAc D1R antagonism does not affect indices of general locomotor activity. a, Rates of active nosepokes made for BLA-to-NAc stimulation early in the behavioral session following intra-NAc vehicle or SCH23390. Rates of active nosepokes were comparable for both groups in the first 8 min of the behavioral sessions (~ 12 min after microinjections). **b**, Burst analysis of active nose-pokes made for BLA-to-NAc stimulation following intra-NAc vehicle or SCH23390. All nosepokes with intervals between nosepokes of < 60 s were classified as belonging to a burst. Intra-NAc SCH2390 did not differ significantly in their intra-burst frequency of responding relative to vehicle-treated mice, suggesting that unilateral SCH23390 does not lead to motor-related deficits in performance. **c**, Average cumulative records for port entries, a measure of locomotor activity in mice that received intra-NAc injections of vehicle or SCH23390. **d**, Average port entries were not significantly different between mice that received intra-NAc vehicle or SCH23390.

Stuber et al., Supplementary Figure 9

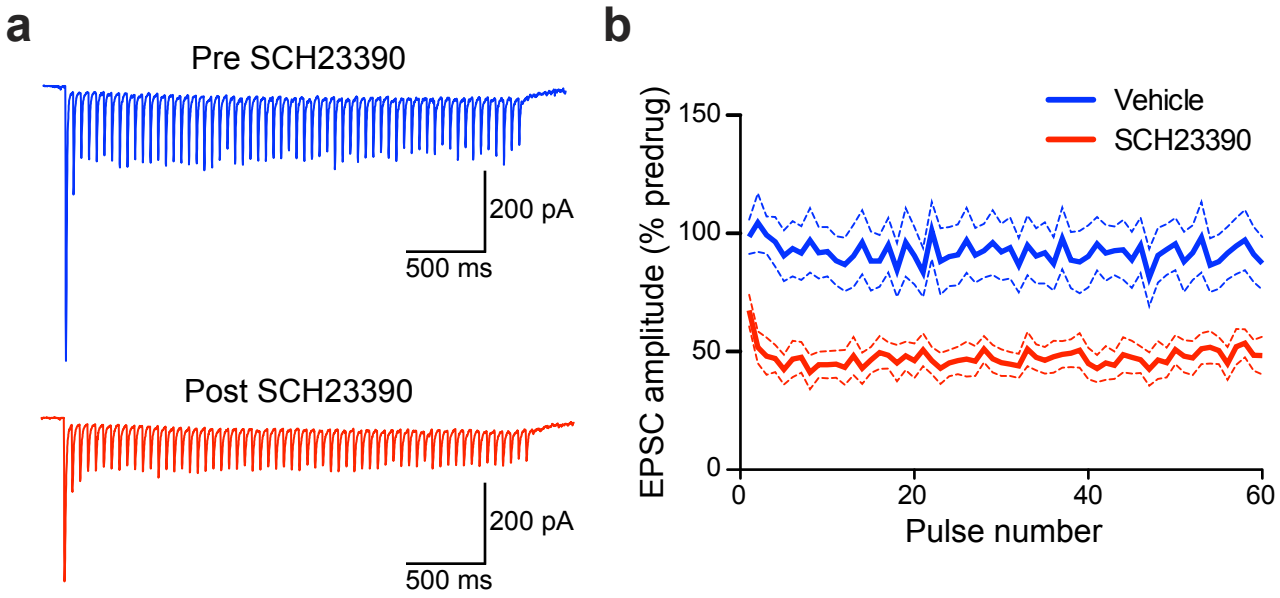

Supplementary Figure 9: Optically stimulated BLA-to-NAc EPSCs are reduced by D1R antagonism *ex vivo*. **a**, Trains of BLA-to-NAc EPSCs before and after bath application of 4 μM SCH23390 evoked by optical stimuli used *in vivo*. **b**, Average EPSC amplitudes for all EPSCs evoked by stimulus train as a function of baseline non-drug-treated values ($F_{59,660} = 701.9$; $P < 0.0001$, n = 7 - 8 cells per group).

Stuber et al., Supplementary Figure 10

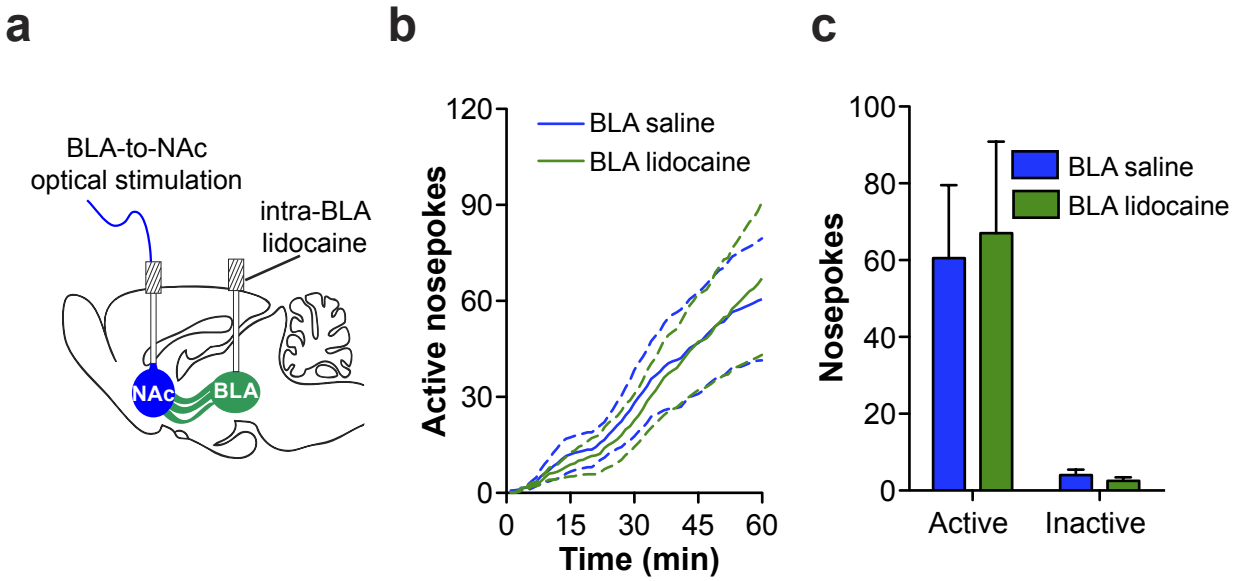

Supplementary Figure 10: Inactivation of BLA does not alter the acquisition of BLA-to-NAc optical self-stimulation. a, Ipsilateral BLA was inactivated by lidocaine injections prior to BLA-to-NAc optical self-stimulation sessions. **b**, Average cumulative active nosepoke records for all mice that received intra-BLA saline or lidocaine immediately prior to their first optical self-stimulation session. **c**, Average active and inactive nosepokes for mice that received intra-BLA saline or lidocaine prior to their first self-stimulation session. Intra-BLA lidocaine did not alter the acquisition of optical self-stimulation (n = 8 per group; *P* = 0.87).

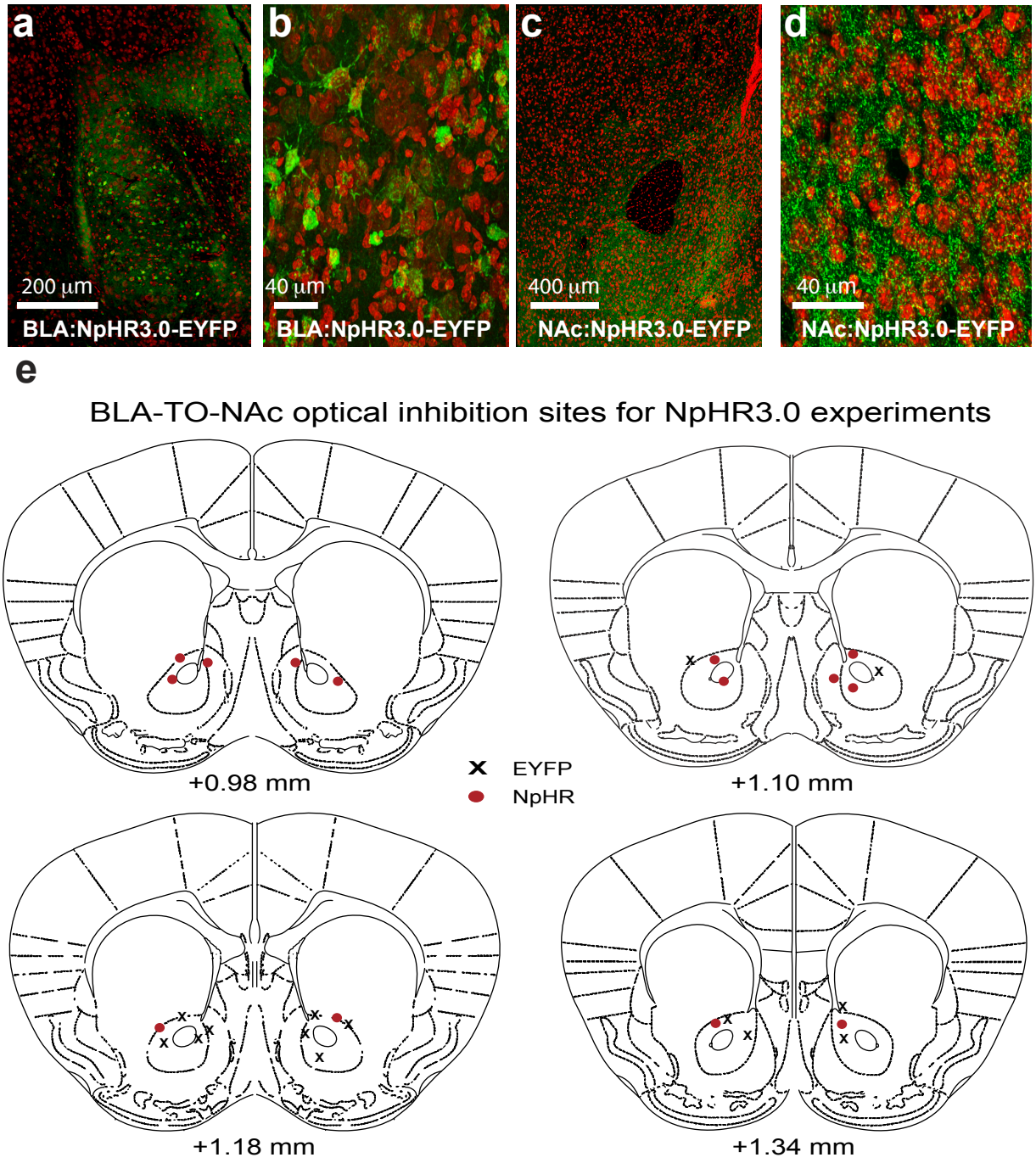

Supplementary Figure 11: NpHR3.0-EYFP expression in the BLA and NAc and optical inhibition sites for BLA-to-NAc expressing NpHR mice. a, Representative image showing expression of NpHR3.0-EYFP in BLA neurons (green). **b**, Higher magnification of the BLA showing NpHR3.0-EYFP expressing neurons (green) **c**, Expression of NpHR3.0-EYFP positive fibers from the BLA innervting the NAc. **d**, Higher magnification of the NAc showing NpHR3.0-EYFP fibers (green) intermixed with postsynaptic neurons (red) **e,** Diagram depicting optical inhibition sites located 0.5 mm from the fiber tip locations for NpHR-EYFP and EYFP used in BLA-to-NAc inhibition experiments.

Stuber et al., Supplementary Figure 12

a

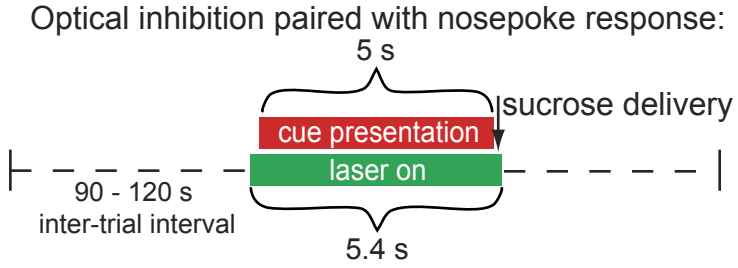

Supplementary Figure 12: Timing diagram of illustrating laser pulse relative to reward- predictive cues and sucrose delivery. **a**, Following a variable inter-trial interval, onset of 532 nm light delivered to the NAc occurred 200 ms prior to onset of the reward-predictive tone/houselight cue (on at t = 0, lasting 5 s). Immediately following the offset of the cue, 20 µl of 20% sucrose was delivered to a receptacle. 200 ms after cue offset, the laser was turned off.

Stuber et al., Supplementary Figure 13

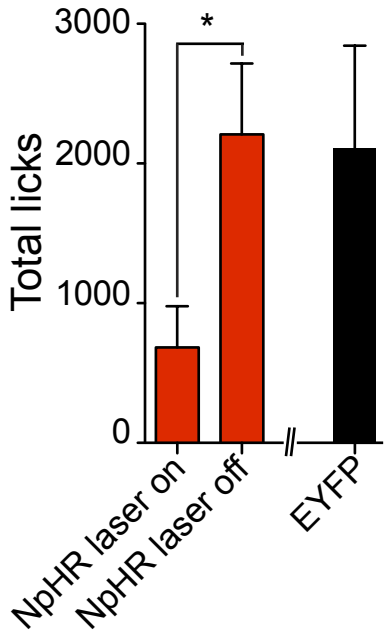

Supplementary Figure 13: Average total licks during NpHR inhibition and non-inhibition. Total number of licks were reduced in sessions where NpHR-expressing mice received optical inhibition compared to sessions where the BLA-to-NAc pathways was unperturbed (*P* = 0.044, n = 7 mice per group).

Stuber et al., Supplementary Figure 14

a

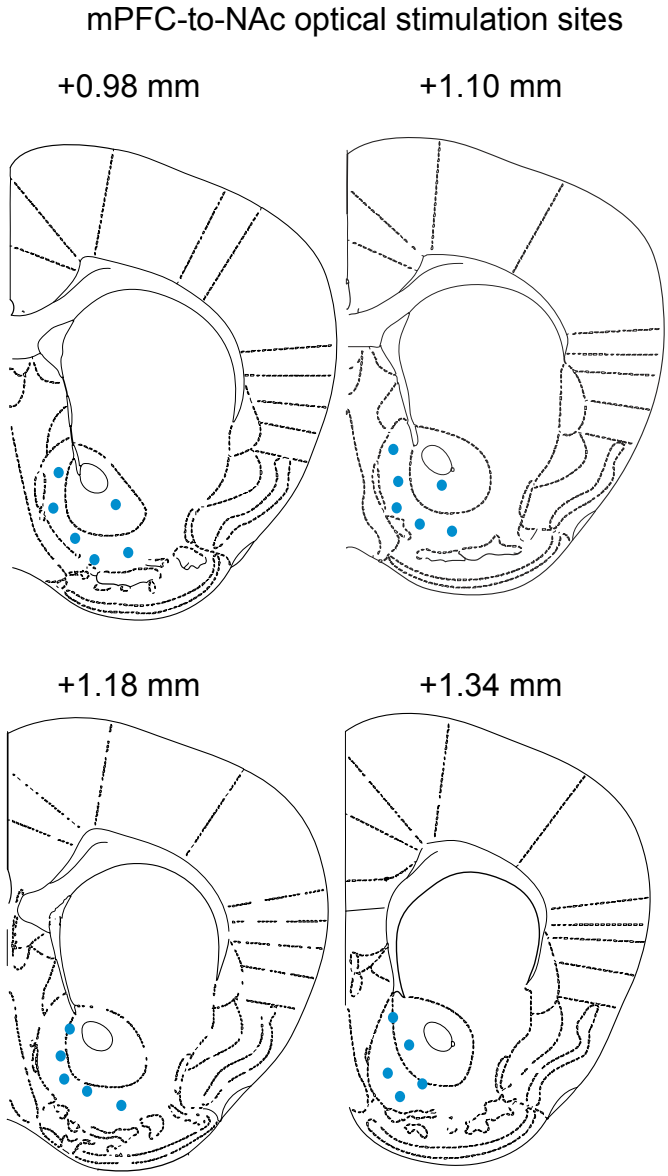

Supplementary Figure 14: Optical stimulation sites for mPFC-to-NAc mice. a, Diagram illustrating optical stimulation sites located 1mm from the cannula tip locations for ChR2-EYFP and EYFP mice used in mPFC-to-NAc stimulation experiments.

Stuber et al., Supplementary Figure 15

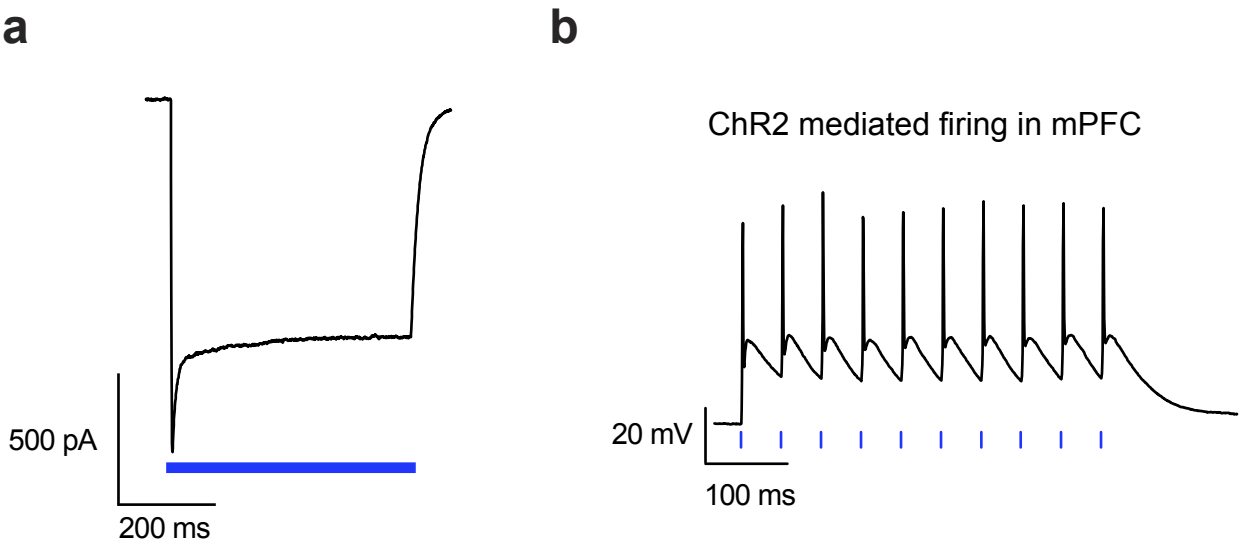

Supplementary Figure 15: mPFC neurons transduced with AAV-CaMKIIa-ChR2-EYFP are optically excitable. **a**, mPFC neurons voltage clamped at -70 mV showed prominent transient and steady-state inward currents in response to 500 ms, 20 mW, 473 nm light application. **b**, Optically-induced firing of mPFC neurons in current-clamp mode at 20 Hz.

Stuber et al., Supplementary Figure 16

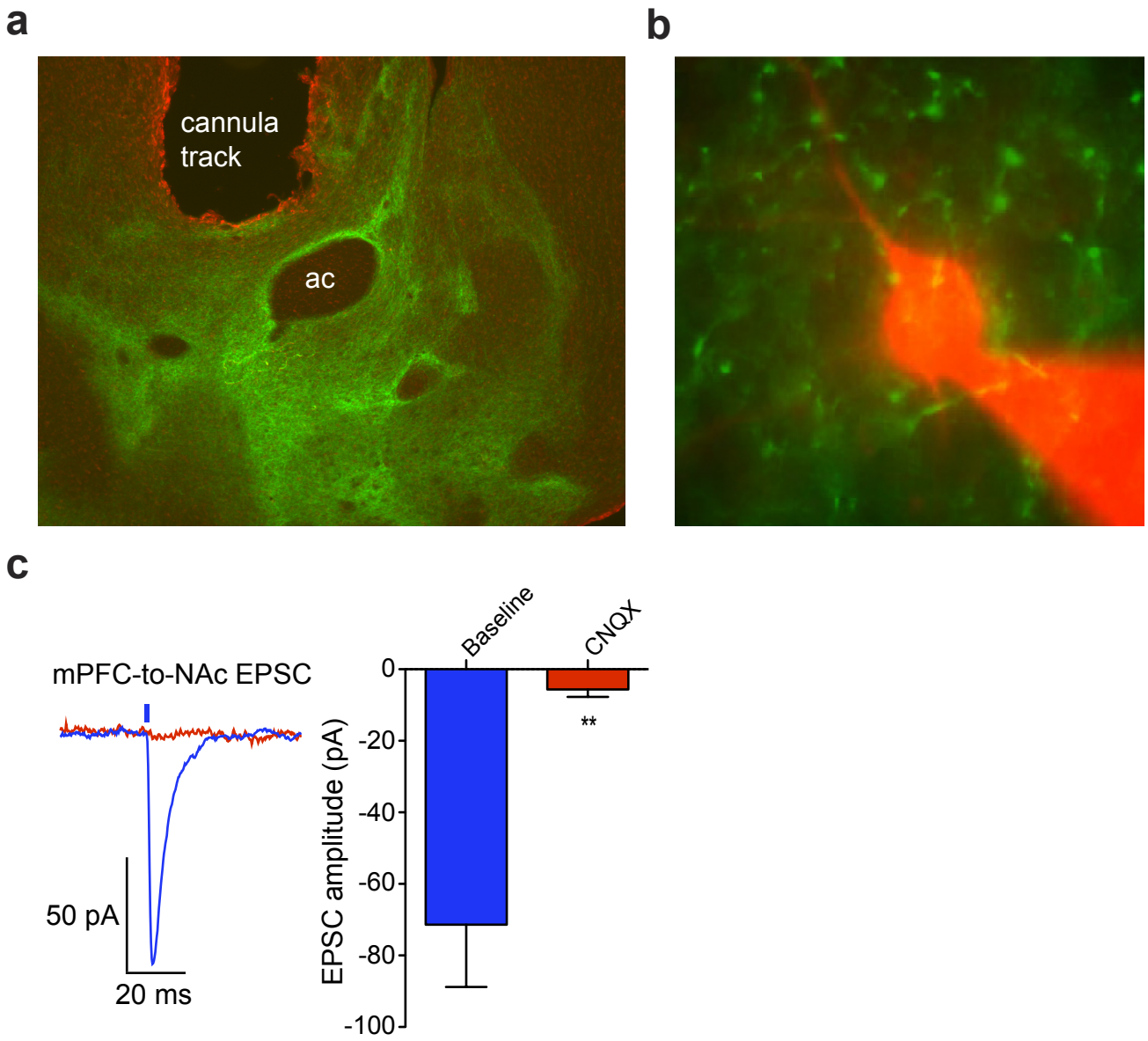

Supplementary Figure 16: Schematic of neurons patched in the NAc in close proximity to guide cannula and mPFC-to-NAc EPSCs. **a**, Image of a brain slice with cannula track expressing ChR2-EYFP at mPFC-to-NAc fibers. Patch-clamp experiments in MSNs while stimulating mPFC-to-NAc synapses were conducted < 200 µm ventral to the end of the guide cannula. ac: anterior commissure. **b**, Image showing a voltage-clamped MSN filled with Alexa-red biocytin in close proximity to the end of the guide cannula also surrounded by ChR2-EYFP positive fibers and terminals originating from the mPFC. **c**, Average EPSC amplitudes evoked following stimulation of mPFC-to-NAc pathway. EPSCs were significantly reduced by bath application of 10 µM ($F(1,56) = 9.63$; $P = 0.003$, n = 7 cells per group).

Stuber et al., Supplementary Figure 17

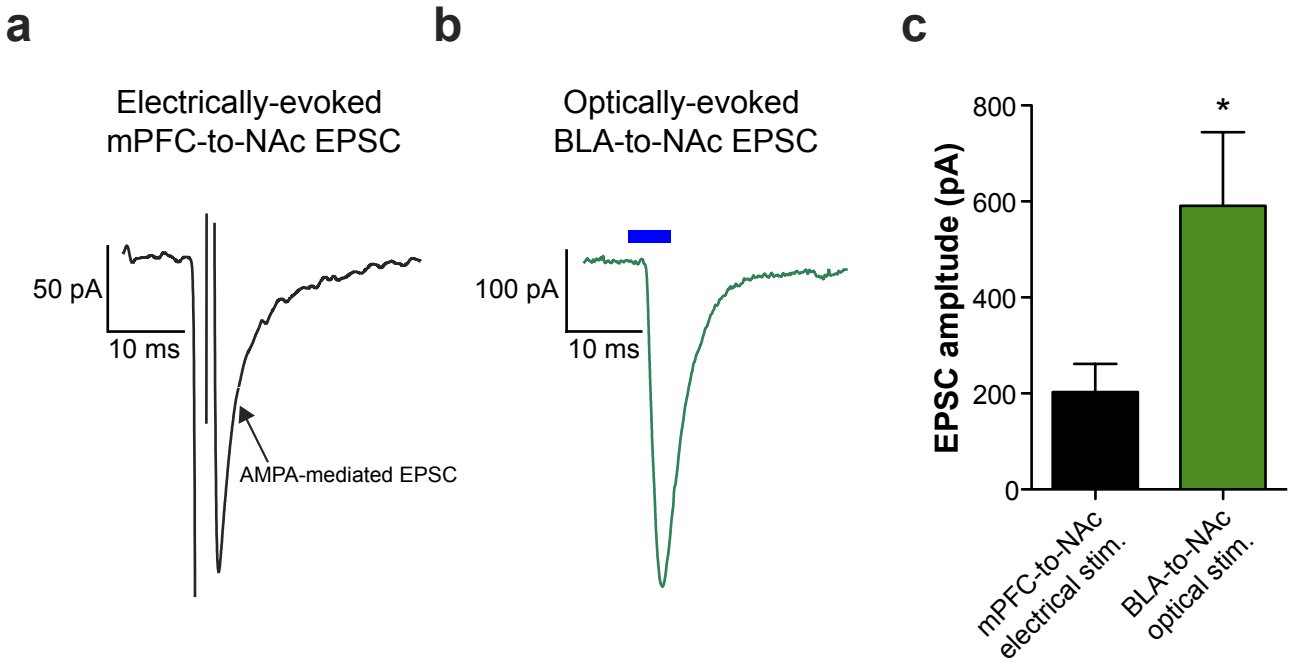

Supplementary Figure 17: Individual NAc MSNs receive both cortical and BLA excitatory inputs **a**, EPSC evoked by electrical stimulation of cortical afferents to the NAc. The electrical stimulating electrode was placed dorsal to the corpus callosum above the NAc. **b**, BLA-to-NAc optically-evoked EPSC from the same neuron. **c**, Average EPSC amplitudes in cells that responded to both optical stimulation of BLA-to-NAc fibers and electrical stimulation of cortical afferents (n = 10). Similiar to optically-evoked data presented in **Fig. 4**, BLA-to-NAc evoked EPSCs were significantly larger than those evoked by stimulation of cortical afferents to the NAc (mPFC-to-NAc electrical stim: 203.1 ± 58.8 pA; BLA-to-NAc optical stim: 591.2 ± 152.8 pA; t(9) = 2.7; *P* = 0.03).